Macromolecules 1987, *20*, 1046–1052

Dilute Solution Physical Properties of Organosilane Polymers

P. M. Cotts* and R. D. Miller

IBM Almaden Research Center, San Jose, California 95120-6099

P. T. Trefonas III and R. West

University of Wisconsin, Madison, Wisconsin 53706

G. N. Fickes

University of Nevada, Reno, Nevada 89557. *Received August 8, 1986*

ABSTRACT: Preliminary light scattering measurements have been carried out on the organopolysilanes $[(n\text{-}C_3H_7)CH_3Si]_n$, $(C_6H_5CH_3Si)_n$, $[(c\text{-}C_6H_{11})CH_3Si]_n$, $[(n\text{-}C_8H_{17})_2Si]_n$, and $[(n\text{-}C_6H_{13})_2Si]_n$ in hexane, cyclohexane, and tetrahydrofuran. For the latter two samples measurements were carried out at various molecular weights. Very high molecular weights (10^6) and correspondingly large molecular dimensions (100 nm) in dilute solution may be observed for these polymers. Chain dimensions (R_G and R_H) together with molecular weights from light scattering indicate that the polysilanes are substantially more extended than carbon backbone polymers of similar degrees of polymerization. Hydrodynamic properties were determined in hexane by dynamic light scattering and viscometry for $[(n\text{-}C_6H_{13})_2Si]_n$, which behaves as a flexible coil in this solvent.

Introduction

Substituted silane high polymers[1] represent a new class of radiation-sensitive materials for which a number of recent applications have been discovered. In this regard, these materials have been utilized as thermal precursors to silicon carbide,[2] as photoinitiators in vinyl polymerizations,[3] and in photoresist applications.[4] The electronic spectra of polysilane derivatives are very unusual in that they absorb strongly in the UV in spite of the fact that the backbone is comprised solely of saturated σ links. This absorption, which depends on both the substituents and the molecular weight,[5] has been described variously as a $\sigma\sigma^*$ or a σ Si^{3d} transition.[6] Since there is considerable σ delocalization in the backbone, the electronic absorption should be dependent on the backbone conformation,[7] and recent studies both in the solid state[8] and in solution suggest[9,10] that this is the case.

The presence of two large aliphatic and/or aromatic groups on each atom of the all-Si backbone produces a chain with highly hindered rotational freedom about the backbone Si–Si bonds. The variation in rotational freedom with substituent is reflected both in the glass transition temperature, T_g, and in the wavelength of maximum ultraviolet absorption, λ_{max}. Parameters that reflect the overall molecular dimensions such as the root-mean-square radius of gyration R_G and the hydrodynamic radius R_H are also expected to be larger than observed for carbon backbone polymers of similar degree of polymerization due to the rigidity arising from the hindrance to rotation. Static light scattering measurements of five polysilanes with varying substituents were used to determine the weight-average molecular weight, M_w, the root-mean-square z-averaged radius of gyration, $R_{G,z}$, and the second virial coefficient A_2. Measurements were carried out in good solvents for the polymers, including hexane, cyclohexane, and tetrahydrofuran. These parameters were used with information about the molecular weight distribution from size exclusion chromatography to estimate the unperturbed dimensions, $R_{G,0}$, for a series of substituents. Two samples, poly(di-*n*-octylsilane) (hereafter abbreviated $[(n\text{-}C_8H_{17})_2Si]_n$) and poly(di-*n*-hexylsilane) ($[(n\text{-}C_6H_{13})_2Si]_n$), were selected for more detailed study. The molecular weight dependence of R_G was investigated by permitting the photolytic degradation of these samples by room light. Hydrodynamic properties of $[(n\text{-}C_6H_{13})_2Si]_n$ were determined in hexane with dynamic light scattering and viscometry.

Table I
Differential Refractive Index Increments

polymer	solvent	λ, nm	T, °C	dn/dc,[a] mL/g
$[(n\text{-}C_3H_7)CH_3Si]_n$	THF	546.1	22.3[b]	0.200
$[(c\text{-}C_6H_{11})CH_3Si]_n$	cyclohexane	546.1	22.3[b]	0.167
$[(n\text{-}C_6H_{13})_2Si]_n$	THF	546.1	22.3[b]	0.106
$[(n\text{-}C_6H_{13})_2Si]_n$	THF	632.8	25.0[b]	0.085
$[(n\text{-}C_6H_{13})_2Si]_n$	hexane	632.8	25.0[c]	0.121
$[(n\text{-}C_8H_{17})_2Si]_n$	THF	632.8	25.0[c]	0.119
$(C_6H_5CH_3Si)_n$	THF	632.8	25.0[c]	0.296

[a] ±0.005. [b] ±0.5 °C. [c] ±0.2 °C.

Experimental Section

Static Light Scattering. Static light scattering measurements were accomplished with three light scattering instruments: (1) SOFICA Model 42000 photogoniometer (University of Wisconsin), (2) Chromatix (LDC Milton Roy) KMX-6 low-angle light scattering photometer (IBM), and (3) Brookhaven BI-200 SM photogoniometer (IBM). Measurements with the SOFICA were done with 546-nm light from a Hg vapor lamp at ambient temperature. Measurements with the KMX-6 and Brookhaven instruments were done with 632.8-nm light from He–Ne lasers (Melles Griot LHP121 and Spectra-Physics 124B, respectively) at 25.0 ± 0.2 °C.

Solutions measured with the KMX-6 were clarified by filtration through 0.5-μm fluoropore filters (Millipore Corp.) directly into the cell of the KMX-6 using a flow-through assembly of Teflon tubing and a syringe pump. Samples were prepared for the Brookhaven instrument by filtration through 0.5-μm disposable filters (Millex HV, Millipore) into cylindrical cells that had been cleaned by refluxing in 2-propanol. Solutions for the SOFICA were clarified by filtration through 0.5-μm Millipore filters directly into the scattering cell.

Differential refractive index increments (dn/dc) at 546.1 and 632.8 nm were measured with a Brice Phoenix differential refractometer (University of Wisconsin) or a Chromatix (LDC Milton Roy) KMX-16 differential refractometer (IBM), respectively. The results for all polymer solvent samples measured are in Table I. The Brice Phoenix instrument was calibrated with aqueous sucrose solutions (dn/dc = 0.001 43 at 546.1 nm at 23 °C)[11] and the KMX-16 was calibrated with aqueous sodium chloride solutions (dn/dc = 0.174 at 632.8 nm and 25.0 °C).[12] The

0024-9297/87/2220-1046$01.50/0

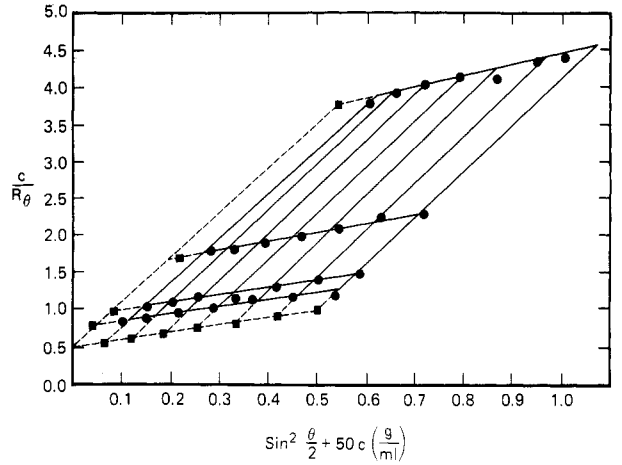

Figure 1. Zimm plot of the elastic light scattering from solutions of $[(c\text{-}C_6H_{11})CH_3Si]_n$ in cyclohexane at 23 °C obtained with the SOFICA. Circles are experimental data and squares are the values obtained by extrapolation to zero angle or zero concentration.

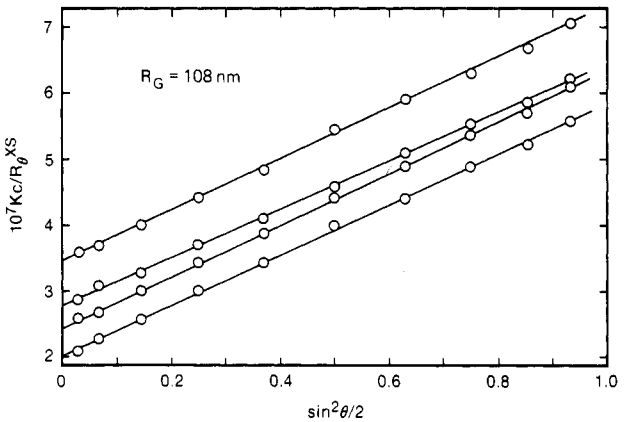

Figure 2. Angular dependence of the elastic light scattering from solutions of $[(n\text{-}C_6H_{13})_2Si]_n$ in hexane at 25 °C obtained with the Brookhaven goniometer from 20° to 150° scattering angle.

parameters M_w, $R_{G,z}$, and A_2 were determined by extrapolation of Kc/R_θ to $\theta = 0$ and $c = 0$ as is indicated by the relation

$$\frac{Kc}{R_\theta} = \frac{1}{M_w}(1 + 2A_2c + 3A_3c^2 + ...)\left(1 + \frac{q^2R_{G,z}^2}{3} + ...\right) \quad (1)$$

with

$$K = \frac{4\pi^2n^2(dn/dc)^2}{N_A\lambda_0^4}$$

and

$$q = \frac{4\pi n}{\lambda_0}\sin(\theta/2)$$

R_θ is the Rayleigh factor at scattering angle θ, c is the concentration in g/mL, n is the refractive index of the solution, N_A is Avogadro's number, and λ_0 is the wavelength of the incident light in vacuum.

In the KMX-6, R_θ is measured directly. For the Brookhaven instrument toluene was used as a reference solvent, using $R_\theta = 14.0 \times 10^{-6}$ cm^{-1} for 632.8-nm light. For the SOFICA, benzene was used, with $R_\theta = 15.8 \times 10^{-6}$ cm^{-1} at 546 nm.

Simultaneous extrapolation of Kc/R_θ to zero scattering angle and infinite dilution were accomplished with a Zimm plot[11] as shown in Figure 1 for $[(c\text{-}C_6H_{11})CH_3Si]_n$. For the very high molecular weight samples, the intramolecular interference factor, $P(\theta)$, can no longer be expressed in its linear limiting form used in eq 1 above

$$P(\theta) = 1 - \frac{q^2R_{G,z}^2}{3}$$

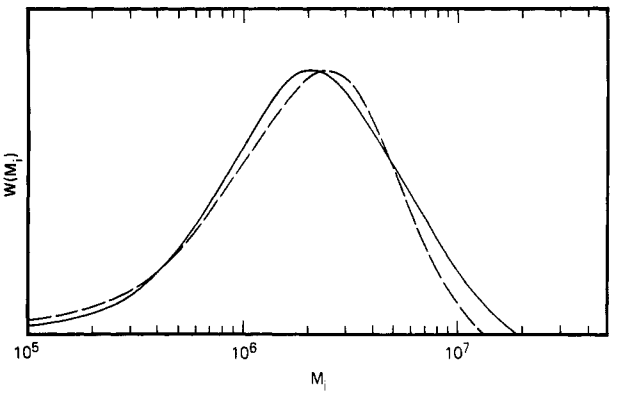

Figure 3. Comparison of the experimental chromatogram obtained for $[(n\text{-}C_8H_{17})_2Si]_n$ in THF with SEC (solid line) with the calculated most probable (Zimm–Schulz) distribution (dashed line).

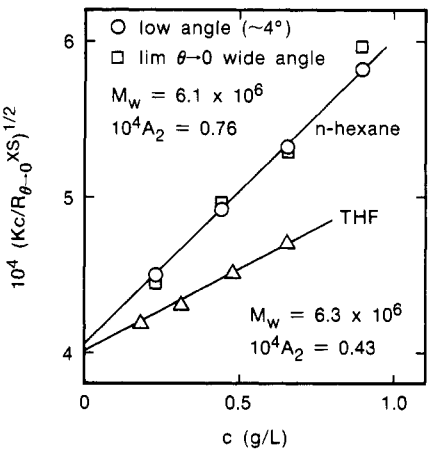

Figure 4. Concentration dependence of the zero-angle elastic scattering from solutions of $[(n\text{-}C_6H_{13})_2Si]_n$ in hexane and THF at 25 °C.

which is valid for small values of $q^2R_{G,z}^2$, and a plot of Kc/R_θ vs. q^2 is expected to cuve upward. However, experimental data on a high molecular weight sample of $[(n\text{-}C_6H_{13})_2Si]_n$, such as that shown in Figure 2, demonstrate that Kc/R_θ is linearly dependent on q^2 even at high scattering angles. This is due to the compensating effect of sample polydispersity, which, for the most probable distribution, leads to an expression for the average $P(\theta)$ that is linear in $q^2R_G^2$ as shown by Zimm[13]

$$P(\theta)^{-1} = 1 + \tfrac{1}{2}\langle q^2R_G^2\rangle_w$$

The most probable distribution is a close approximation of the experimental distribution obtained for the high M sample of $[(n\text{-}C_8H_{17})_2Si]_n$ as shown in Figure 3. Determination of M_w and A_2 for the high molecular weight samples was accomplished with a square-root plot of $(Kc/R_0)^{1/2}$ vs. c where the subscript 0 indicates extrapolation to zero scattering angle. Measurements with the KMX-6 at $\theta = 4.4°$ were equivalent to the extrapolated zero-angle ones determined with the Brookhaven goniometer at $20° < \theta < 150°$, as shown in Figure 4. The square root plot has been suggested to minimize extrapolation errors for high molecular weight polymers in good solvents where higher order terms in the virial expansion may contribute to the concentration dependence.[14-16]

The depolarization ratio, ρ_v, is given by

$$\rho_v \equiv R_{Hv}/R_{Vv}$$

where R_{Hv} and R_{Vv} are the limiting Rayleigh factors of the light scattered at zero angle from a vertically polarized source with horizontally and vertically polarized analysers, respectively. Values of ρ_v varied from 0.0017 to 0.0023 for solutions of $[(n\text{-}C_6H_{13})_2Si]_n$ in hexane, so that corrections due to optical anisotropy were negligible.

Table II
Molecular Parameters of Organosilane Polymers

polymer	solvent	M_w^{LS}	10^4A_2	R_G, nm	M_w/M_n	M_w^{PS} [a]
$[(n\text{-}C_3H_7)CH_3Si]_n$	THF	210 000 ± 50 000	2.2 ± 0.5	31 ± 5	3.1 ± 0.3	180 000
$[(c\text{-}C_6H_{11})CH_3Si]_n$	cyclohexane	2 540 000 ± 500 000	1.2 ± 0.2	76 ± 8	2.7 ± 0.3	800 000
$[(n\text{-}C_6H_{13})_2Si]_n$	cyclohexane	7 400 000 ± 500 000	0.5 ± 0.1	102 ± 15	1.3 ± 0.7	2 200 000
$[(n\text{-}C_6H_{13})_2Si]_n$	hexane	6 100 000 ± 500 000	0.8 ± 0.1	108 ± 15	2.3 ± 0.3	1 900 000
$[(n\text{-}C_6H_{13})_2Si]_n$	THF	6 300 000 ± 500 000	0.4 ± 0.1	92 ± 15	2.3 ± 0.3	1 900 000
$[(n\text{-}C_8H_{17})_2Si]_n$	THF	3 200 000 ± 500 000	1.0 ± 0.2	100 ± 15	2.4 ± 0.3	2 600 000
$(C_6H_5CH_3Si)_n$	THF	46 000 ± 10 000	3.6 ± 0.5	21 ± 5	4.2 ± 0.3	19 000

[a] These values are relative to polystyrene as discussed in text.

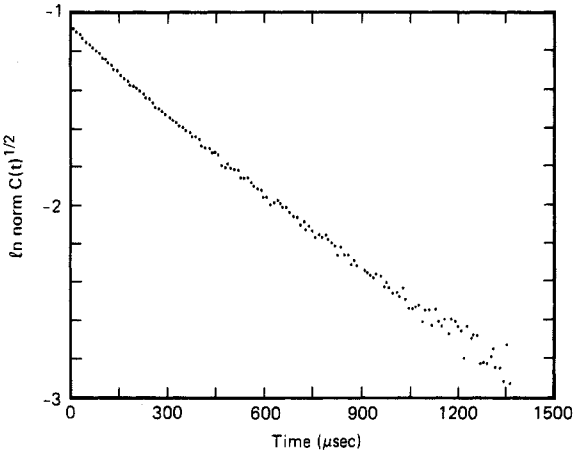

Figure 5. The log of the square root of the normalized correlation function (see eq 2 in text) vs. time for $[(n\text{-}C_6H_{11})_2Si]_n$ in hexane.

Dynamic Light Scattering. Dynamic light scattering was measured with the Brookhaven 200 SM photogoniometer equipped with a BI2030 128-channel correlator to measure the time correlation function $C(t)$, which was analyzed by the method of cumulants[17]

$$\ln\left(\frac{C(t)}{B} - 1\right)^{1/2} = \ln b^{1/2} - \Gamma t + \mu_2 t^2/2 + \ldots \qquad (2)$$

with B the base line of the correlation function and b an optical constant. The diffusion coefficient D_c at each concentration c is obtained from the extrapolation of the reduced first cumulant, $D_c(q) \equiv \Gamma_{c,q}/q^2$, to zero scattering angle

$$D_{z,c} = \lim_{q\to 0} (\Gamma_{c,q}/q^2)$$

The normalized second cumulant, μ_2/Γ^2, which reduces to zero for a purely single-exponential decay, describes the deviation from a single exponential arising from polydispersity or other relaxations. The sample time Δt was selected with the criterion

$$\Delta t = 2/(m\Gamma)$$

with m the number of channels.

This criterion for selecting a sample time provides a large number of channels in the initial decay at the expense of longer time data. Thus a greater precision in the first cumulant is obtained while the second cumulant may be quite imprecise. The second cumulant is difficult is measure and interpret and we rely here on size exclusion chromatography to obtain a measure of polydispersity. A normalized correlation function is shown in Figure 5. We have used a measured base line (average of four delay channels 1029–1032 times the sample time Δt) as B; however, the calculated base line (infinite time value) and measured base line agreed within 0.1% for all measurements used.

Viscometry and Size Exclusion Chromatography. The intrinsic viscosity, $[\eta]$, of poly(di-*n*-hexylsilane) in hexane was measured with a Cannon Ubbelohde semimicroviscometer equipped with a Wescan automatic viscosity timer. $[\eta]$ was determined by extrapolation of the reduced viscosity, η_{sp}/c and the inherent viscosity, $\ln \eta_{rel}/c$ to infinite dilution, as shown in Figure 6, using the Huggins and Kramers relations

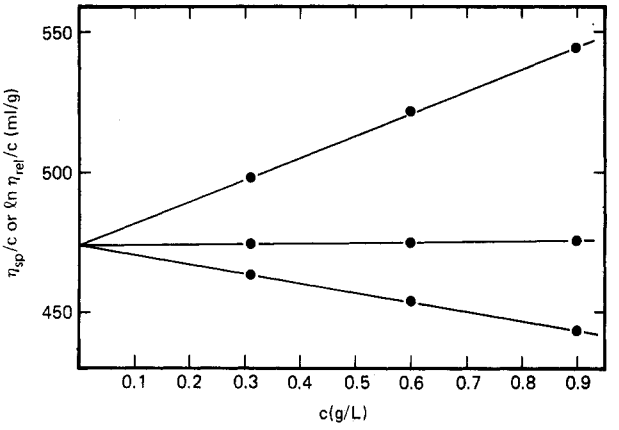

Figure 6. Reduced viscosity, η_{sp}/c, and the inherent viscosity, $\ln \eta_{rel}/c$, as a function of concentration for $[(n\text{-}C_6H_{13})_2Si]_n$ in hexane at 20 °C.

$$\frac{\eta_{sp}}{c} = \frac{\eta_{rel} - 1}{c} = [\eta] + k[\eta]^2 c + \ldots$$

and

$$\frac{\ln \eta_{rel}}{c} = [\eta] - (1/2 - k)[\eta]^2 c + \ldots$$

with $\eta_{rel} = \eta/\eta_0$ with η and η_0 the viscosities of the solution and solvent, respectively. $[\eta] \equiv 474$ mL/g and the Huggins coefficient k was 0.357, similar to values usually observed for flexible polymers in good solvents. Although kinetic energy corrections are expected to be very small at these flow times, significant deviation from the limiting $[\eta]$ at zero shear rate may be possible at the high molecular weight used and this was not assessed.

Size exclusion chromatography was used to estimate the polydispersity of each sample. A total of 150 μL of each sample at a concentration of approximately 1 mg/mL was injected onto a set of four mixed gel columns (ASI Ultragel), using tetrahydrofuran (THF) as the mobile phase and a differential refractometer as the concentration detector. The column set was calibrated with a series of narrow distribution polystyrene standards (Polymer Laboratories) and a calibration curve was fit to a third-order polynomial

$$\log M = A + Bt + Ct^2 + Dt^3$$

where t is the peak elution time of a PS standard of molecular weight M. Calculation of apparent molecular weight averages relative to polystyrene, M_w^{PS}, M_n^{PS}, M_z^{PS} and the polydispersity (M_w^{PS}/M_n^{PS}) were carried out with an IBM PCXT with chromatography software (Nelson Analytical). An example of a typical distribution obtained is shown in Figure 3 for $[(n\text{-}C_8H_{17})_2Si]_n$.

Results and Discussion

Static Light Scattering. The molecular parameters obtained from static light scattering, M_w, $R_{G,z}$, and A_2, are listed in Table II for the various polysilanes studied. The polydispersity, M_w/M_n, and the molecular weight relative to the polystyrene calibration, M_w^{PS}, obtained from size

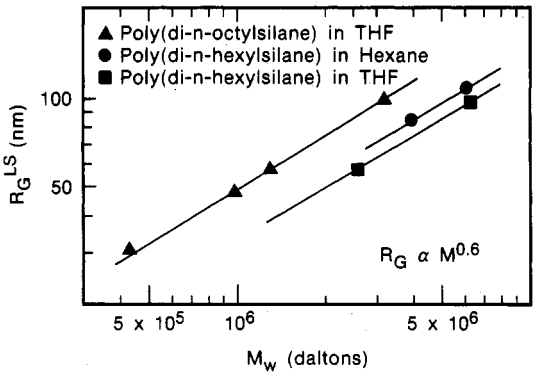

Figure 7. Dependence of the root-mean-square radius of gyration from light scattering, R_G^{LS}, on M_w for series of $[(n\text{-}C_6H_{13})_2Si]_n$ and $[(n\text{-}C_8H_{17})_2Si]_n$ obtained by photolytic degradation in THF and hexane.

exclusion chromatography, are also listed. It is apparent that very high molecular weights may be obtained for these polymers. The apparent molecular weights M_w^{PS} obtained by SEC cannot be directly compared with true weight-average molecular weights determined by light scattering. For the very high molecular weight samples of $[(n\text{-}C_8H_{17})_2Si]_n$ and $[(n\text{-}C_6H_{13})_2Si]_n$, the elution times of the samples approached the exclusion limit of the columns used, so that these values of M_w^{PS} are more uncertain. Due to the difficulty in synthesizing a range of molecular weights, the molecular weight dependence of R_G was investigated for $[(n\text{-}C_8H_{17})_2Si]_n$ and $[(n\text{-}C_6H_{13})_2Si]_n$ by permitting photochemical degradation in room light. This degradation in M was sufficiently slow to permit measurement of M_w and R_G as the samples degraded, as shown in Figure 7.

During the measurement, each sample was exposed to room light for approximately 5–10 min. The scattered intensity did not decrease significantly during this time, despite the high sensitivity of scattered intensity to small changes in molecular weight. The degradation to the lower molecular weights displayed in Figure 7 required exposure of solutions to room light over a period of 2 weeks. The exponent ν in the relation

$$R_G \propto M^{\nu}$$

is equal to 0.62 as is observed for flexible coil polymers in good solvents. Random chain scission is expected to lead to a normal distribution not substantially different from the original distribution of these samples, so that the exponent of 0.62 would also be expected for a series of narrow distribution samples. The exponent of 0.62 is direct evidence for the coillike configuration of the polymer chain. The larger R_G obtained in hexane is consistent with the larger A_2 measured in this solvent and suggests that excluded volume effects are significant in spite of the highly hindered rotational freedom.

The linearity of the $P^{-1}(\theta)$ function for $0° < \theta < 150°$ permits the use of the KMX-6 to estimate R_G from measurements at only two angles, 4.4° and 175.6°, analogous to dissymmetry measurements used early in light scattering experiments. This technique requires experimental evidence for the linearity of the $P^{-1}(\theta)$ function such as that shown in Figure 2 since the presence of large scattering species, such as dust or aggregates, or large polydispersity can introduce significant curvature that cannot be assessed with measurement at only two angles. The KMX-6 provides a degree of precision (±0.2%) that we have not been able to attain with the more traditional goniometer. Measurement of R_G using this "dissymmetry" method over a range of concentrations for $[(n\text{-}C_6H_{13})_2Si]_n$ in hexane

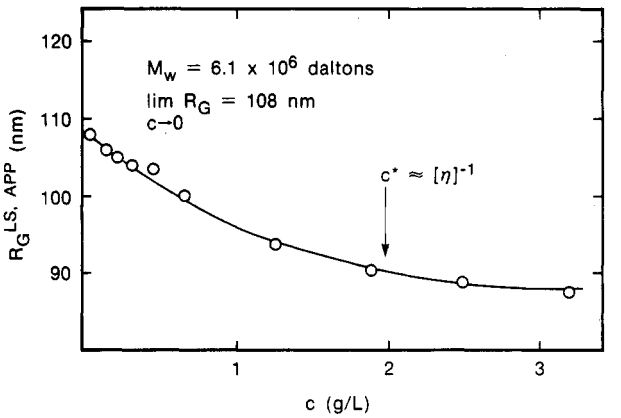

Figure 8. Decrease in $R_G^{LS,APP}$ with concentration for $[(n\text{-}C_6H_{13})_2Si]_n$ in hexane.

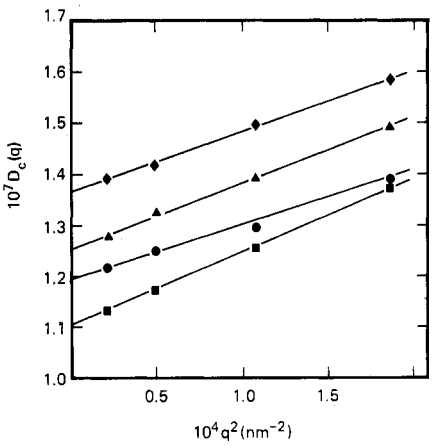

Figure 9. Reduced first cumulant, $D_c(q) \equiv \Gamma/q^2$ obtained from cumulant analysis of dynamic light scattering as a function of q^2 for four concentrations of $[(n\text{-}C_6H_{13})_2Si]_n$ in hexane at 25 °C.

showed a decrease in R_G with increasing concentration, as is shown in Figure 8. The decrease in R_G with increasing concentration in dilute solution due to competing intramolecular and intermolecular interactions has been predicted[18–21] and confirmed by neutron scattering measurements.[22] For light scattering, determination of R_G at a finite concentration c requires the assumption that the function $Q(\theta)$ representing the intermolecular interference in the more complete expression of eq 1

$$\frac{K_c}{R_\theta} = \frac{1}{M_w P(\theta)} + 2A_2 Q(\theta)c + \ldots$$

is negligible; i.e., $Q(\theta)$ is nearly unity. Since the observed decrease in R_G in Figure 8 is very similar to that observed by Jannink et al.[20] using neutron scattering, this assumption appears to be reasonable.

Dynamic Light Scattering. The reduced first cumulant $D_c(q)$ method of cumulants (eq 2, above) is shown as a function of q^2 for several concentrations of $[(n\text{-}C_6H_{13})_2Si]_n$ in hexane in Figure 9. In the small q limit the q^2 dependence is linear as expected for diffusive motion. Measurements were carried out at scattering angles θ = 20, 30, 45, and 60°. Values of the normalized second cumulant μ_2/Γ^2 were 0.17 ± 0.04 and were independent of angle and concentration in this range. In the low-q region ($qR_G < 1$) the magnitude of μ_2/Γ^2 reflects the polydispersity of the sample. The polydispersity determined from dynamic light scattering may be compared with that obtained from SEC, provided the exponent ν in the relation

$$D \propto M^{-\nu}$$

is known. Here we use $\nu = 0.6$ based on the measurements

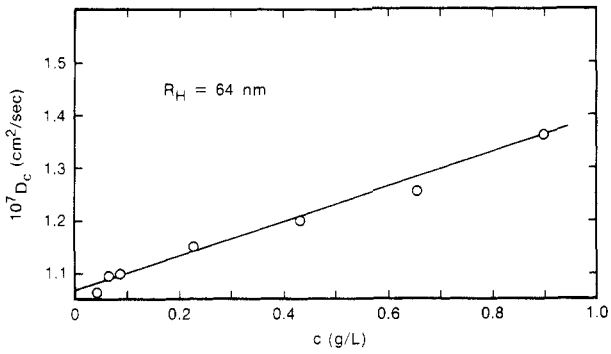

Figure 10. Concentration dependence of D_c obtained from extrapolation of $D_c(q)$ to zero angle for $[(n\text{-}C_6H_{13})_2Si]_n$ in hexane.

of R_G of photolytically degraded samples discussed above. Substitution of $\nu = 0.6$ and $\delta \equiv M_w/M_n - 1 = 1.3$ (see Table II) into the expression[23]

$$\frac{\mu_2}{\Gamma^2} = \frac{\nu^2}{4}\frac{\delta[4 + (1-\nu)(\nu-5)\delta]}{[1 + [(2-\nu)(1-\nu)/2]\delta]^2}$$

yields $\mu_2/\Gamma^2 = 0.11$ in comparison with the experimental value of 0.17 ± 0.04 for $[(n\text{-}C_6H_{13})_2Si]_n$. Above 60° scattering angle ($qR_G > 1$) the deviation from a single exponential became more significant, indicating contributions from internal motions of the chain. The concentration dependence of D_c is shown in Figure 10 and may be expressed as

$$D_c = D_0(1 + k_D c)$$

with $D_0 = (1.07 \pm 0.05) \times 10^{-7}$ cm²/s and $k_D = 290 \pm 30$ cm³/g. The hydrodynamic radius, R_H, defined by the Einstein relation for a hard sphere

$$D_0 = \frac{kT}{6\pi\eta_0 R_H}$$

is 67 ± 3 nm. The hard-sphere value for A_2, which may be appropriate in the good solvent limit, is given by

$$A_2 = \frac{4N_A}{M_w^2}V_H$$

where V_H is the hydrodynamic volume of the sphere

$$V_H = \tfrac{4}{3}\pi R_H^3$$

and may be compared with the experimental A_2. We obtain $10^4 A_2 = 0.7 \pm 0.1$ mL/(g mol) in good agreement with the experimental value of $10^4 A_2 = 0.8 \pm 0.1$ mL/(g mol) measured by static light scattering for $[(n\text{-}C_6H_{13})_2Si]_n$ in hexane. This agreement suggests that the polymer coil behaves thermodynamically as well as hydrodynamically like a hard sphere of radius R_H, which is also observed for polystyrene and other flexible polymers in good solvents. The concentration dependence k_D of the diffusion coefficient may also be expressed in volume fraction units

$$k_D{}^\Phi = \frac{M_w}{N_A V_H}k_D$$

which yields $k_D{}^\Phi = 2.7$ in reasonable agreement with the Yamakawa prediction of 2.2 for the good solvent limit.[24]

The ratio $R_G/R_H = 1.7 \pm 0.1$ is in good agreement with the prediction of 1.73 for polydisperse flexible coils with a most probable distribution.[25] R_H and R_G may be compared with a radius $R_{G,\eta}$ calculated from the intrinsic viscosity $[\eta]$ using the Fox–Flory equation[26]

$$[\eta] = \frac{6^{3/2}\Phi R_{G,\eta}^3}{M_w}$$

where Φ is the Flory viscosity constant, 2.5×10^{23} for polydisperse samples with infinite hydrodynamic interaction. For $[(n\text{-}C_6H_{13})_2Si]_n$ in hexane, $[\eta] = 474 \pm 10$ mL/g at 20 °C, so that $R_{G,\eta} = 90 \pm 1$ nm. The intrinsic viscosity $[\eta]$ measures an average that is close to a weight average, so that $R_{G,\eta}$ is expected to be smaller than $R_{G,z}$ determined by light scattering by a factor that may be estimated to be 0.83 based on the SEC results for M_z/M_w. The experimental ratio $R_{G,\eta}/R_{G,z} = 0.83$, in excellent agreement with the SEC results. Although the first cumulant from dynamic light scattering on polydisperse molecules measures a z-average diffusion coefficient

$$\langle D\rangle_z = \sum w_i M_i D_i / M_w$$

the inverse relation of D to M results in the hydrodynamic radius R_H being most closely related to that obtained for a monodisperse sample with the same M_w rather than M_z. The hydrodynamic radius R_H calculated from the first cumulant may be compared directly with $R_{G,\eta}$, since both measurements yield an average that is close to a weight average. The ratio $R_{G,\eta}/R_H = 1.41$, which is quite consistent with the value of 1.50 predicted for monodisperse chains in the nondraining limit (infinite hydrodynamic interaction).

Estimation of Unperturbed Chain Dimensions. The light scattering data in Table II may be used to estimate the characteristic ratio, C_∞, or alternatively the ratio $(R^0_{G,w})^2/M_w$, which may be compared with values for other polymers to assess the flexibility of the chain. The superscript 0 indicates a measurement at Θ conditions where excluded volume effects are absent, and the subscript w indicates a correction of the measured $R_{G,Z}$ to an average appropriate for comparison with M_w, i.e., such that

$$\frac{(R^0_{G,w})^2}{M_w} \cong \frac{(R^0_G)^2}{M} \tag{3}$$

where the parameters on the right-hand side of eq 3 are determined for a narrow distribution fraction. Since $R_G \propto M^{0.6}$

$$\frac{R_{G,z}}{R_{G,w}} \propto \left(\frac{M_z}{M_w}\right)^{0.6}$$

Correction of $R_{G,w}$ for expansion due to excluded volume requires an estimate of the expansion factor

$$\alpha \equiv R_G/R^0_G$$

This may be obtained from various approximate theories that relate α and the interpenetration function ψ, where[16]

$$\psi = \frac{A_2 M_w^2}{4\pi^{3/2}N_A R_{G,w}^3}$$

Experimental values of ψ are listed in Table III, and are very large for the high molecular weight samples of $[(n\text{-}C_6H_{13})_2Si]_n$ and $[(n\text{-}C_8H_{17})_2Si]_n$. Various theories predict an upper limit on ψ of 0.2–0.3 and, experimentally, values larger than 0.3 are rarely observed for flexible chain polymers.[16] The limited number of samples and large values of ψ make estimation of the magnitude of the excluded volume effect very approximate. Use of the available theories for ψ and α and experimental data obtained for other flexible polymers[14] lead to estimates of $\alpha \cong 1.3 \pm 0.3$ for $[(n\text{-}C_6H_{13})_2Si]_n$ in hexane. An empirical relation between the experimental parameter $A_2 M_w/[\eta]$ and $\alpha^2 - 1$ also leads to an estimate of ~1.3 for α for $[(n\text{-}C_6H_{13})_2Si]_n$ in hexane.[16] Using these expressions and the information about the polydispersity listed in Table I, we obtain the values for $R^0_{G,w}$ and N_w shown in Table III,

Table III
Estimation of Unperturbed Dimensions

polymer	N_w	solvent	ψ	$R_{G,w}^0$, nm	C_∞
$[(n\text{-}C_3H_7)CH_3Si]_n$[a]	2500 ± 500	THF	0.07 ± 0.05	21 ± 10	19 ± 7
$[(c\text{-}C_6H_{11})CH_3Si]_n$	20000 ± 4000	cyclohexane	0.15 ± 0.05	50 ± 10	14 ± 5
$[(n\text{-}C_6H_{13})_2Si]_n$	37000 ± 2500	cyclohexane	0.25 ± 0.05	87 ± 10	21 ± 5
$[(n\text{-}C_6H_{13})_2Si]_n$	31000 ± 2500	hexane	0.30 ± 0.05	77 ± 10	20 ± 5
$[(n\text{-}C_6H_{13})_2Si]_n$	31000 ± 2500	THF	0.20 ± 0.05	76 ± 10	20 ± 5
$[(n\text{-}C_8H_{17})_2Si]_n$	12600 ± 2000	THF	0.15 ± 0.05	59 ± 10	30 ± 5
$(C_6H_5)CH_3Si)_n$	400 ± 75	THF	0 ± 0.05	15 ± 10	64 ± 20

[a] These showed a small secondary peak in the SEC chromatogram in the high-M region.

where N_w is the weight-average number of backbone chain atoms. The values of $(R_{G,w}^0)^2/N_w$ are 15–30 (with dimensions in angstroms), substantially larger than the values of 2–4 observed for typical carbon backbone polymers such as polystyrene, poly(methyl methacrylate), etc. The characteristic ratio, C_∞, where

$$C_\infty = \frac{\langle r^2\rangle_0}{Nl^2}$$

with $\langle r^2\rangle_0$ the mean square end-to-end distance and l the length of the Si–Si bond, 2.35 Å, may also be calculated. We assume that $\langle r^2\rangle_0 \cong 6(R_{G,w}^0)^2$ as for Gaussian chains and obtain the values listed in Table III. For the poly(di-n-hexylsilane), $C_\infty \cong 20$, which is larger than the value of 10 obtained for polystyrene for example.

The values of $R_{G,w}^0$ and C_∞ obtained for the samples other than $[(n\text{-}C_6H_{13})_2Si]_n$ are less certain due to the limited measurements. In particular some samples contained a small high molecular weight fraction which can have a very large effect on $R_{G,z}$ measured by light scattering. The agreement among the measurements of the poly(di-n-hexylsilane) for the different solvents and instruments used and the agreement with hydrodynamic measurements discussed above substantially improve the reliability of C_∞ for this sample; however as discussed above, estimation of the magnitude of the excluded volume effect is very uncertain. Measurements in a Θ-solvent are required before a definitive conclusion about the flexibility of these polymers can be made.

Although it appears that the $[(n\text{-}C_6H_{13})_2Si]_n$ chain is quite flexible, at least by equilibrium measurements, we can estimate the persistence length ρ with the Kratky–Porod model.[28] Near the coil limit, ρ may be determined by solving simultaneous expressions for the contour length L and R_G^2 in terms of equivalent Kuhn segments l_k

$$L = nl_k$$

$$R_G^2 = \tfrac{1}{6}nl_k^2$$

The contour length L is estimated as $N_w l$ where N_w is the number of backbone Si atoms and l is the projection of the Si–Si bond onto the backbone, 1.94 Å. The persistence length $\rho = l_k/2$. For $[(n\text{-}C_6H_{13})_2Si]_n$ we obtain $l_k = 5.8 \pm 0.7$ nm and $\rho = 2.9 \pm 0.3$ nm, using the value of $R_{G,w}^0$ listed in Table III. Use of experimentally determined $R_{G,z}$ from light scattering, without correction for polydispersity and excluded volume effects, leads to a much larger estimate for the persistence length ρ. Although estimates for these corrections are uncertain, they are reinforced by agreement with hydrodynamic dimensions obtained with independent techniques.

Chain dimensions (R_G and R_H) and molecular weights obtained from light scattering indicate that the polysilanes are substantially more extended than carbon-backbone polymers of similar degree of polymerization. This increase in size is due to the longer Si–Si bond length and to the highly substituted backbone which provides a large degree of steric hindrance to rotation. Despite the large dimensions, the chains appear to behave as flexible coils at the very high molecular weights studied. This is evidenced by the exponent of 0.62 in the relation of R_G to M and by the decrease in R_G of the $[(n\text{-}C_6H_{13})_2Si]_n$ in the poorer solvent THF relative to the R_G obtained in hexane. The question of whether the chains obey Gaussian statistics with an exponent of 0.5 in a Θ-solvent where excluded volume effects are absent awaits measurements in a Θ-solvent. The temperature dependence of the overall chain dimensions, which has been suggested undergoes a low-temperature transition,[9,10] is also being investigated.[29]

Acknowledgment. R.D.M gratefully acknowledges partial financial support by the Office of Naval Research.

Registry No. $[(n\text{-}C_3H_7)CH_3Si]_n$, 88003-13-8; $[(c\text{-}C_6H_{11})CH_3Si]_n$, 88003-16-1; $[(n\text{-}C_6H_{13})_2Si]_n$, 94904-85-5; $[(n\text{-}C_8H_{17})_2Si]_n$, 98865-30-6; $[C_6H_5CH_3Si]_n$, 76188-55-1.

References and Notes

(1) (a) For reviews of polysilanes, see: West, R. *J. Organometallic Chem.* **1986**, *300*, 327. (b) West, R. "Organopolysilanes" In *Comprehensive Organometallic Chemistry*; Abel, E., Ed.; Pergamon: Oxford, England, 1982; Chapter 9.4, pp 365–397.
(2) (a) Yajima, S.; Hasegawa, Y.; Hayaski, Y.; Imura, M. *J. Mater. Sci.* **1975**, *13*, 2569. (b) Hasegawa, Y.; Imura, M.; Yajima, S. *J. Mater. Sci.* **1978**, *15*, 2569.
(3) West, R.; Wolff, A. R.; Peterson, D. J. *J. Radiat. Curing* **1986**, *13*, 35. Wolff, A. R.; West, R. *Appl. Organomet. Chem.*, in press.
(4) (a) Miller, R. D.; Hofer, D.; McKean, D. R.; Willson, C. G.; West, R.; Trefonas, P., III, In *Materials for Microlithography*; Willson, C. G., Frêchet, J. M. J., Eds.; American Chemical Society; Washington, D.C., 1984; *ACS Symp. Ser. No. 266*. (b) Hofer, D. C.; Miller, R. D.; Willson, C. G. *Proc. SPIE Adv. Resist Technol.* **1984**, *469*, 108. (c) Hofer, D. C.; Miller, R. D.; Willson, C. G. *Ibid.* 16.
(5) Trefonas, P., III; West, R.; Miller, R. D.; Hofer, D. *J. Polym. Sci., Polym. Lett. Ed.* **1983**, *21*, 823.
(6) Pitt, C. G. In *Homoatomic Rings, Chains and Macromolecules of the Main Group Elements*, Rheingold, A. L., Ed.; Elsevier: New York, 1977.
(7) Bock, H.; Ensslin, W.; Fêher, F.; Freund, R. *J. Am. Chem. Soc.* **1976**, *98*, 668.
(8) Miller, R. D.; Hofer, D.; Rabolt, J. F.; Fickes, G. N. *J. Am. Chem. Soc.* **1985**, *107*, 2172.
(9) Trefonas, P., III; Damewood, J. R., Jr.; West, R.; Miller, R. D. *Organometallics* **1985**, *4*, 1318.
(10) Harrah, L. A.; Zeigler, J. M. *J. Polym. Sci., Polym. Lett. Ed.* **1985**, *23*, 209.
(11) Maron, S. H.; Lou, R. L. H. *J. Phys. Chem.* **1955**, *59*, 231.
(12) Kruis, A. *Z. Phys. Chem., Abt. B* **1936**, *34*, 13.
(13) Zimm, B. H. *J. Chem. Phys.* **1948**, *16*, 1093; **1948**, *16*, 1099.
(14) Flory, P. J. *Principles of Polymer Chemistry*; Cornell University: Ithaca, NY, 1953; Chapter VII.
(15) Berry, G. C. *J. Chem. Phys.* **1966**, *44*, 4550.
(16) Yamakawa, H. *Modern Theory of Polymer Solutions*; Harper and Row: New York, 1971; Chapter VII.
(17) Koppel, D. E. *J. Chem. Phys.* **1972**, *57*, 4814.
(18) Fixman, M.; Peterson, J. M. *J. Am. Chem. Soc.* **1964**, *86*, 3524.
(19) Graessley, W. *Polymer* **1980**, *21*, 258.
(20) Sanchez, I. C.; Lohse, D. J. *Macromolecules* **1981**, *14*, 131.
(21) Akcasu, A. Z.; Hammouda, B. *Macromolecules* **1983**, *16*, 951.
(22) Jannink, G. et al. *Macromolecules* **1975**, *8*, 804.
(23) Selser, J. *Macromolecules* **1979**, *12*, 909.

(24) Yamakawa, H. J. Chem. Phys. 1962, 36, 2995.
(25) Frenker, I.; Burchard, W. Macromolecules 1973, 6, 848.
(26) Flory, P. J.; Fox, T. G., Jr. J. Am. Chem. Soc. 1951, 73, 1904.
(27) Flory, P. J. Statistical Mechanics of Chain Molecules, Wiley-Interscience: New York, 1969; Chapter I.
(28) Kratky, O.; Porod, G. Recl. Trav. Chim. Pays-Bas 1949, 68, 1106.
(29) Cotts, P. M. Proceedings of Polymeric Materials, Science and Engineering Division; American Chemical Society: Washington, D.C., 1985; Vol. 53, p 336.

Liquid-Expanded to Liquid-Condensed Phase Transition in Polyelectrolyte Monolayers on the Aqueous KBr Solution. 1. Salt Concentration Dependence

Masami Kawaguchi,* Sadanori Itoh, and Akira Takahashi

Department of Industrial Chemistry, Faculty of Engineering, Mie University, 1515 Kamihama-cho, Tsu, Mie 514, Japan. *Received September 4, 1986*

ABSTRACT: Fully quaternized poly(vinylpyridinium bromides) with three different *n*-alkyl chains were prepared by spontaneous polymerization. The surface pressure of the quaternized polymer monolayers spread at the air–water interface was measured as a function of KBr concentration. In the surface pressure (π)–surface area (A) (π–A) isotherm the absolutely flat portion corresponding to so-called liquid-expanded to liquid-condensed transition is simply a first-order transition for each polymer. At smaller A the π–A curves can be superimposed independent of the *n*-alkyl chain length and KBr concentration. The limiting area estimated from an extrapolation of the straight portion on the π–A isotherm to $\pi = 0$ shows that the pyridinium rings are attached flat on the water surface while hydrocarbon side chains are oriented vertically. Additional measurement of interfacial pressure of the quaternized polymer monolayer at the *n*-heptane–water interface demonstrates that the small negative cooperative cohesive energy (attractive force) mainly governs the existence of the flat portions in π–A isotherms. Qualitative comparison with some theoretical works can interpret the interfacial behavior of a polyion monolayer at the air–water interface.

Two-dimensional charged insoluble monolayers spread at the air–water interface are interesting from a fundamental and a practical point of view. Particularly, intensive attention has been paid to the two-dimensional phase transition. Two prominent phase transitions are well understood to occur in the surface pressure–surface area (π–A) isotherms under appropriate surrounding conditions, for example, temperature and salt concentration of water subphase. Most works on the phase transition have concentrated on fatty acid and phospholipid monolayers.[1,2] The so-called gas–liquid (G–L) transition at lower surface pressure is generally accepted to be a first-order transition. Another transition at higher surface pressure is usually denoted liquid-expanded to liquid-condensed (LE–LC) phase change. It was usually observed that the LE–LC transition occurs as a single slope change in the π–A isotherm. However, more recently Pethica and co-workers observed a completely horizontal portion in π–A isotherms of the LE–LC transition in fatty acids and phospholipid monolayers.[3,4]

Due to high solubillity in water and difficulty in forming films on the water surface, studies on polyelectrolyte monolayers have been lacking in comparison with nonionic polymer monolayers. To conquer this limitation several attempts have been performed by preparing (1) polymers with partially ionized chains such as random[5] and block[6,7] copolymers and (2) quaternized poly(vinylpyridine) with alkyl halides.[8]

Plaisance and Ter-Minassian-Saraga[8] systematically measured the surface pressure of poly(2-vinyl-5-methylpyridine) quaternized with hexyl or octyl bromide monolayers spread at the air–aqueous salt solution interfaces. Their π–A isotherms showed a dramatic change with variation of ionic strength or salt species, and the LE–LC transition was observed for the specific salts. However, they did not deeply study the LE–LC transition. Moreover, their samples were not fully quaternized.

In general, the 100% quaternization of poly(vinylpyridine) with *n*-alkyl halides was not attained if the *n*-alkyl chain length was long.[9] On the other hand, a mixture of 4-vinylpyridine and *n*-alkyl halide in a given solvent leads to the 100% quaternized poly(4-vinylpyridinium) salt by spontaneous polymerization[10] accompanied with the quaternization or protonation of the 4-vinylpyridine monomer.

In this paper we prepare fully quaternized poly(4-vinylpyridinium) salts from the spontaneous polymerization of 4-vinylpyridine and three different *n*-alkyl bromides. Surface pressure measurements of the resulting polyelectrolyte monolayers spread on aqueous KBr solutions are performed as a function of KBr concentration. The characteristics of their π–A isotherms will be discussed, focusing on the LE–LC transition as a function of *n*-alkyl chain length and KBr concentration.

Experimental Section

Materials. Poly(4-vinylpyridines) (PVP) quaternized with three different *n*-alkyl bromides such as *n*-hexyl bromide, *n*-octyl bromide, and *n*-dodecyl bromide were prepared by the spontaneous polymerization[10] of freshly distilled 4-vinylpyridine and *n*-alkyl bromide in distilled dimethyl cellosolve at around −15 °C. Three *n*-alkyl bromides were used without further purification. Reaction time was about $^1/_2$ year. With an increase in reaction time, quaternized polymers were precipitated. The product was washed several times by a large amount of dimethyl cellosolve. The polymers separated by filtration were dissolved in methanol and precipitated into excess distilled water. An additional dissolution (in methanol) and precipitation (in water) sequence was repeated to purify the polymers. They were dried under vacuum to remove water at room temperature.

The degree of the quaternization in the polymers was checked by elementary analysis.

Number-average molecular weights of the polymers were determined with a Knauer vapor pressure osmometer in methanol at 30 °C.

0024-9297/87/2220-1052$01.50/0